

Electromechanical responses of single-walled carbon nanotubes: Interplay between the strain-induced energy-gap opening and the pinning of the Fermi level

G. Y. Guo

Department of Physics, National Taiwan University, Taipei 106, Taiwan

Lei Liu

Department of Physics, University of Louisville, Louisville, Kentucky 40292

K. C. Chu

Department of Physics, National Taiwan University, Taipei 106, Taiwan

C. S. Jayanthi and S. Y. Wu^{a)}

Department of Physics, University of Louisville, Louisville, Kentucky 40292

(Received 14 March 2005; accepted 6 July 2005; published online 19 August 2005)

A comprehensive picture of electromechanical responses of carbon single-walled nanotubes (SWNTs) is obtained using *ab initio* density-functional theory and self-consistent π -orbital Hamiltonian. We find a linear behavior of the energy gap of zigzag SWNTs as a function of the axial strain with different slopes for compression versus extension. Observed small changes in conductance even with a substantial energy gap due to the strain is attributed to the pinning of the Fermi level near the top of the valence band. © 2005 American Institute of Physics. [DOI: 10.1063/1.2011781]

I. INTRODUCTION

Mechanical manipulation of carbon single-walled nanotubes (SWNTs) is expected to provide a means to functionalize the properties of nanotubes (NTs). For example, the pioneering experiment of Tomblor *et al.* showed a reversible two-orders-of-magnitude reduction of conductance of a freely suspended metallic SWNT when it is deflected by an atomic force microscope (AFM) tip at a relatively small angle.¹ More recently, Minot *et al.*, using an AFM tip that can simultaneously strain and gate the NT, demonstrated that while the change in conductance associated with the axial strain (up to a strain of $\sim 2\%$) in a SWNT is relatively small, gating it locally via the AFM tip can enhance the change up to about one order of magnitude.² Theoretically, Liu *et al.* attributed the observed reversible two-order-of-magnitude reduction in conductance due to the AFM deflection of a metallic SWNT at a relatively small angle to a reversible sp^2 to sp^3 bonding transition of the carbon atoms adjacent to the AFM tip, based on a careful simulation using a nonorthogonal tight-binding/molecular-dynamics (NOTB/MD) scheme.³ On the other hand, Maiti *et al.* argued that the opening of an energy gap in an axially stretched SWNT might result in a two-order-of-magnitude reduction in conductance.⁴ This conclusion, however, is apparently contrary to the observation of Minot *et al.*² Experimental evidences^{2,5} and theoretical expectations⁶⁻⁸ seem to give strong support of the gap opening in the band structure of metallic SWNTs under an axial stretching. Therefore, there must be additional factors at play that lead to the observation of only small changes in conductance for strain up to $\sim 2\%$ in spite of appreciable opening of

the energy gap. One likely candidate is the pinning of the Fermi level in the vicinity of highest occupied molecular orbital (HOMO) [or lowest unoccupied molecular orbital (LUMO)] due to the finite length of the sample SWNT between the contacts.

In this paper, we present the result of our detailed study of the effect of the change in the band structure due to an axial strain on the transport properties of SWNTs to clarify and settle issues raised by experimental observations. Using the accurate full-potential projector augmented-wave (PAW) method⁹ as implemented in the VASP package,¹⁰ we calculated the energy gap of axially stretched zigzag SWNTs of various sizes to provide the most reliable determination of the gap opening as a function of the strength of the axial strain. We found that with increasing elongation, the energy gap of semimetallic zigzag SWNTs initially decreases linearly, vanishes at a small strain, and thereafter starts to increase linearly at a smaller slope (compared to the decreasing slope) for strains with strength up to $\sim 3\%$. Our calculation indicated that the energy gap of stretched zigzag SWNTs could be as great as a few hundred meV. For example, for the (27,0) SWNT under a 2% strain, the energy gap opens to ~ 250 meV. With the energy gap of this magnitude, the most likely cause for the observed small changes in conductance associated with axial strains of up to $\sim 2\%$ could only be the pinning of the Fermi level in the immediate vicinity of either the valence band or the conduction band. Such pinning could indeed occur on account of the finite length of the sample SWNTs (from a few hundred nanometers to a few microns). To confirm this scenario, we determined the effect of the finite size of the sample SWNT on the charge transfer between the sample and the metal leads, and hence the pinning of the Fermi level, using a self-consistent scheme for the

^{a)}Electronic mail: shi-yu.wu@louisville.edu

determination of the charge redistribution based on the π -orbital tight-binding (TB) theory. We found that when the electrons flow from the finite sample SWNT to the leads, the Fermi level is pinned to the vicinity of the top of the valence band. For strains of $\sim 2\%$, we showed that this pinning of the Fermi level is responsible for only small reductions in conductance in axially stretched SWNTs as long as there is no local perturbation such as gating² or deformation via AFM tip.¹ Thus, we have demonstrated conclusively that it is the interplay among the energy-gap opening associated with the strain, the pinning of the Fermi level in the vicinity of either the top of the valence band or the bottom of the conduction band due to the finite length of the SWNT, and the local perturbation that determines the electromechanical responses of SWNTs.

II. THE METHOD

In order to establish how reliable the all-electron PAW method is in predicting electronic properties of SWNTs, we first used it to determine the opening of an energy gap in metallic zigzag SWNTs due to the curvature effect. We decided to calculate the energy gap of semimetallic zigzag SWNTs for the following reasons. (1) The curvature effect is most pronounced for metallic zigzag SWNTs.¹¹ (2) The number of carbon atoms in a unit cell of zigzag SWNTs is smaller compared with that in a unit cell of chiral SWNTs.¹¹ (3) There are experimental measurements of the energy gap in zigzag metallic SWNTs.¹² In our study, we first construct the initial configuration of a given zigzag SWNT by simply wrapping its corresponding graphene strip with the chiral angle $\phi=0$. The equilibrium configuration of the zigzag SWNT is then obtained by relaxing the initial configuration using the PAW method. Finally the electronic structure of the relaxed zigzag SWNT is calculated to determine the opening of the energy gap due to the curvature of the tube. In our PAW calculations, we used density-functional theory (DFT) with local-density approximation (LDA) and the exchange-correlation potential of Ceperley-Alder as parameterized by Perdew and Zunger.¹³ A supercell geometry was adopted so that the nanotubes are aligned in a square array with the closest distance between adjacent nanotubes being at least 8 Å. A uniform k -space grid of $1 \times 1 \times 20$ and a large plane-wave cutoff of 500 eV were used. It should be noted that the lattice constants of graphite determined by the PAW DFT-LDA calculations are in very good agreement with the experimental values (within 0.5%).¹⁴ In Fig. 1, the calculated energy gaps for the series of “semimetallic” zigzag SWNTs (9,0), (12,0), (15,0), ..., (27,0), and (36,0) are plotted vs. the radius of the tube. Also plotted are the available experimental scanning tunneling microscope (STM) measurements of the energy gap.¹² It can be seen that the calculated energy gaps of the unstrained semimetallic zigzag SWNTs are in good agreement with the available experimental results. Furthermore, the functional dependence of the energy gap on the radius r can be seen to follow a $1/r^2$ pattern.

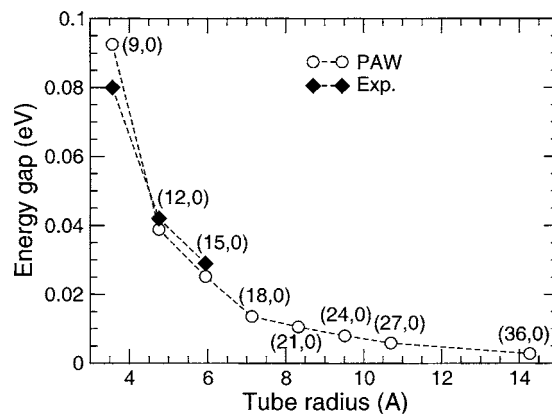


FIG. 1. Calculated (open circles) and experimental (solid diamonds) (Ref. 12) energy gaps of unstrained zigzag semimetallic SWNTs vs their radii.

III. THE ENERGY GAP AND THE AXIAL STRAIN

Having established the validity and the reliability of the PAW method in its prediction of the opening of an energy gap due to the curvature for unstrained semimetallic zigzag SWNTs, we proceeded to employ the same method to determine further change in the energy gap when these SWNTs are axially strained. In our approach, the axial strain with a strength given by $\sigma=(l-l_0)/l_0$ is initially applied to a certain zigzag SWNT, with l_0 being the equilibrium length in the axial direction for the unit cell of the unstrained SWNT and l the corresponding length in the strained tube. The equilibrium configuration of the strained tube is then obtained by relaxation using the PAW method. The energy gap of the strained tube is finally determined by calculating the electronic structure of the equilibrium configuration of the strained tube. Here an accurate DFT-based all-electron theory is used to study the strain effect for semimetallic SWNTs. Figure 2 shows the plot of the energy gap for a subset of the strained semimetallic zigzag SWNTs [(9,0), (12,0), (15,0), and (27,0) NTs] considered in Fig. 1 as a function of the strength of the axial strain. It can be seen that for both the case of stretching and the case of compression, the energy gap for the semimetallic zigzag SWNTs exhibits a linear dependence on the strength of the strain. For stretching, the linear dependence prevails at least to a 3% strain while the linear relation starts to break down beyond a 2%

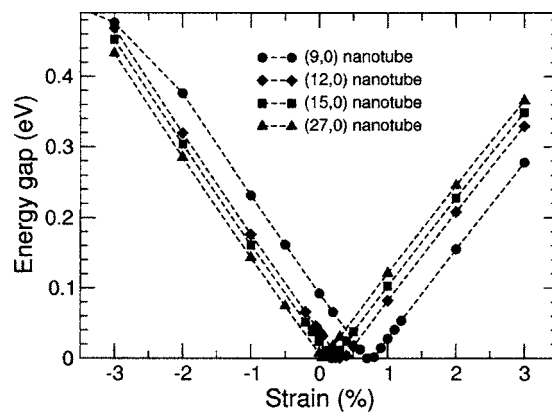


FIG. 2. Calculated energy-gap variation of zigzag (9,0), (12,0), (15,0), and (27,0) SWNTs as a function of axial strain.

strain for compression. As discussed previously, an energy gap opens for unstrained semimetallic SWNTs because of the effect of the curvature. Under an axial stretching, we found that the initial energy gap due to the curvature decreases linearly at first with increasing strain, vanishes at a relatively small strain, and from that point on increases linearly with increasing strain. Viewed from the critical strain σ_{crit} where the energy gap vanishes, the behavior pattern of the change in the energy gap as a function of the strain can be separated into two categories. For a strain $\sigma > \sigma_{\text{crit}}$, the slope of the linear dependence is positive while it is negative for $\sigma < \sigma_{\text{crit}}$. In this sense, the change in the energy gap under compression is an extension of the initial response under stretching where $\sigma < \sigma_{\text{crit}}$, namely, the energy gap of an unstrained SWNT shows a linear increase with increasing compression (more negative strain). Furthermore, the slopes of the linear dependence of the energy gap on the axial strain for all the semimetallic zigzag SWNTs considered are all the same, suggesting that the rate of change of the energy gap with respect to the applied strain is independent of the radius of the SWNTs. Figure 2 also shows that the absolute value of the slope for $\sigma < \sigma_{\text{crit}}$ is greater than that for $\sigma > \sigma_{\text{crit}}$. Our calculation of the rate of change of the energy gap with respect to the strain yields ~ 140 meV/% for $\sigma < \sigma_{\text{crit}}$ and ~ 120 meV/% for $\sigma > \sigma_{\text{crit}}$, compared with an absolute value of ~ 100 meV/% based on the Hückel TB model.^{2,8}

IV. THE PINNING OF THE FERMI LEVEL

Figure 2 indicates that an axial strain can result in an energy gap of a substantial magnitude. For example, under stretching with a 2% strain, the energy gap of a (12,0) zigzag SWNT opens up to ~ 200 meV, compared with an energy gap of only ~ 30 meV due to the curvature for the unstrained (12,0) SWNT. With a change in the energy gap of such magnitude, one would expect an orders-of-magnitude change in the conductance if the Fermi level of the contacted SWNT is in the vicinity of the middle of the gap. Yet experimental measurements mentioned previously detected only relatively small changes for axially strained SWNTs with no local perturbation.² In that experiment, the SWNTs were contacted by gold electrodes.² There were experimental evidences of a *p*-type behavior for SWNTs contacted by gold,^{2,5,15} indicating that the Fermi level is pinned to the vicinity of the top of the valence band. While the pinning of the Fermi level near the top of the valence band may be crucial in explaining the observed small changes in conductance, the physics underlying the pinning is not yet clearly understood. Furthermore, the extent of the pinning and, in particular, how the pinning will be affected by the axial strain needs to be fully understood before a complete picture of the electromechanical responses of SWNTs emerges.

To shed light on the abovementioned issues, we carried out a model study of the redistribution of the charge across the interface between the sample SWNT and the metal leads. Special emphasis was placed on the fact that the length of the sample SWNT is finite. In our model study, we consider a (12,0) SWNT with a length of 10 nm. This sample SWNT is contacted at both ends by metallic leads. The size of the

system under consideration precludes the use of DFT-based methods to calculate the charge transfer between the sample and the leads. Instead, we employ a model Hamiltonian based on the single π -orbital theory that explicitly allows (i) the calculation of the energy-gap opening due to the axial strain and (ii) the self-consistent determination of the charge transfer across the interface. The system Hamiltonian used in our calculation is composed of the sample Hamiltonian (H^S), the Hamiltonian for the leads (H^L), and the Hamiltonian for the interaction between the sample and the lead (H^{int}). The sample Hamiltonian H^S is constructed according to

$$H_{ii}^S = \varepsilon_S + q_i U + e^2 \sum_{k \neq i} \frac{q_k}{r_{ik}}, \quad (1)$$

$$H_{ij}^S = \gamma_0 \left(\frac{d_{ij}^0}{d_{ij}} \right)^2, \quad (2)$$

where ε_S is the orbital energy for the carbon atom, $q_i = N_i - Z_i$ with $N_i e$ being the charge on the *i*th atom and $Z_i = 1$, U a Hubbard-like intra-atomic correlation energy term given by $U = 18.46$ eV,¹⁶ r_{ik} the distance between atoms at site *i* and site *k*, $\gamma_0 = 2.7$ eV the nearest-neighbor off-diagonal Hamiltonian element for the unstrained SWNT in the single π -orbital theory, d_{ij}^0 the bond length between carbon atoms *i* and *j* in the unstrained SWNT, and d_{ij} the corresponding bond length in the strained SWNT. The summation over *k* in Eq. (1) runs through atoms in the sample as well as in the leads because of the long-range Coulomb interaction. The off-diagonal elements of the sample Hamiltonian, H_{ij}^S , are restricted to only the nearest neighbors, as in the single π -orbital theory. The Hamiltonian for the leads is chosen to be

$$H_{ii}^L = \varepsilon_L + q_i U + e^2 \sum_{k \neq i} \frac{q_k}{r_{ik}}, \quad (3)$$

$$H_{ij}^L = \gamma', \quad (4)$$

while the Hamiltonian H_{ij}^{int} between the neighboring atoms in the sample and those in the lead is chosen simply as γ_0 .

The appearance of terms containing q_i , r_{ij} , and d_{ij} in the system Hamiltonian provides the scheme to self-consistently determine the charge transfer for a SWNT under a given axial strain. By satisfying the requirement of the self-consistency in the charge redistribution, the Fermi level of the contacted SWNT under the axial strain is also determined. Thus, the Hamiltonian described in Eqs. (1)–(4) also allows the determination of the pinning of the Fermi level corresponding to a given axial strain. In the calculation, the off-diagonal Hamiltonian element γ' of the lead is set equal to $\gamma_0/20$ to model the metallic nature of the lead. To model the contact between the gold lead and the (12,0) SWNT, ε_L is set equal to zero while ε_S equal to 400 meV to reflect the difference in the work function between the NT and the gold lead so that electrons will flow from the SWNT to the metallic lead. To circumvent the difficulty in the self-consistent process due to the fact that TB formalisms only give the charge at a site, we consider the charge to be uniformly distributed over a unit cell of the SWNT and use the average

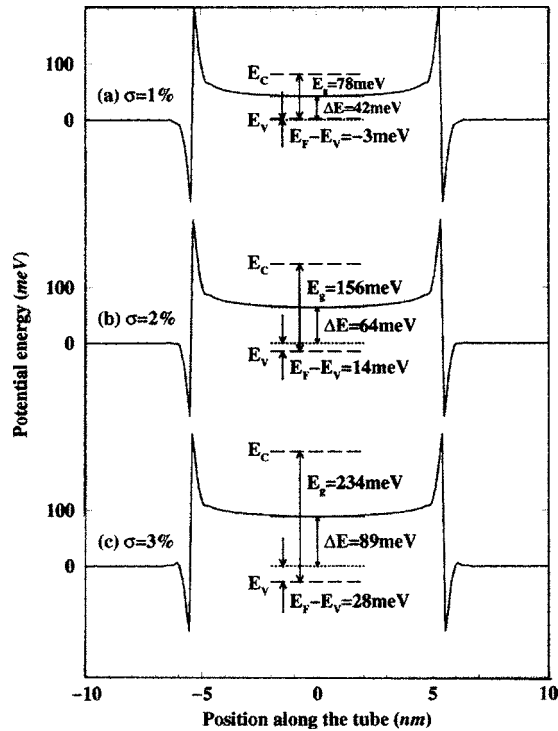


FIG. 3. Self-consistently determined potential energy of zigzag (12,0) SWNT as a function of the atomic position along the tube for (a) strain $\sigma = 1\%$, (b) $\sigma = 2\%$, and (c) $\sigma = 3\%$, respectively. The calculated Fermi levels for the three cases are shown being pinned near the top of the valence band.

charge over a unit cell to achieve the self-consistency in the charge redistribution, a procedure similar to the one used by Léonard and Tersoff.^{17,18}

The result of the determination of the pinning of the Fermi level at a temperature of 300 K for strains $\sigma = 1\%$, 2% , and 3% is summarized in Fig. 3. Specifically, we have plotted the self-consistently determined energy $\varepsilon_{L(S)} + [q_i U + e^2 \Sigma_k (q_k / r_{ik})]$ along the contacted SWNT where the SWNT occupies the position from -5 to 5 nm. Also shown is the band-structure energy in the body of the strained SWNT as it is shifted by the amount of the self-consistent potential energy $\{E_{C(V)} + \varepsilon_S + [q_i U + e^2 \Sigma_k (q_k / r_{ik})]\}$, where $E_{C(V)}$ denotes the bottom (top) of the conduction (valence) band. In the plot, the Fermi level (E_F) is set to zero. It can be seen that the contacted (12,0) SWNT indeed exhibits a p -type behavior with the Fermi level pinned beneath E_V by 3 meV for a strain of 1%, above E_V by 14 meV for a strain of 2%, and by 28 meV for a strain of 3%. We have calculated the conductance of the p -type-behaving strained (12,0) SWNT using

$$\begin{aligned}
 G &= \frac{2e^2}{h} \int_{-\infty}^{\infty} T(E) \left(-\frac{\partial f}{\partial E} \right) dE \\
 &= \frac{2e^2}{h} \left[\int_{-\infty}^{E_F} T(E) \left(-\frac{\partial f}{\partial E} \right) dE + \int_{E_C}^{\infty} T(E) \left(-\frac{\partial f}{\partial E} \right) dE \right] \\
 &\approx \frac{4e^2}{h} \left[\frac{1}{1 + e^{-(E_F - E_V)/kT}} + \frac{1}{1 + e^{(E_C - E_F)/kT}} \right], \quad (5)
 \end{aligned}$$

where $T(E)$ is the transmission coefficient as a function of E and $f(E)$ the Fermi distribution function. At room temperature, we found relatively small changes in conductance of the strained with respect to the unstrained (12,0) SWNT, namely, a factor of 0.6 for a 1%, 0.4 for a 2%, and 0.3 for a 3% strain. This result is consistent with the experimental observation.

V. SUMMARY

In summary, our accurate PAW calculation has clearly established the linear behavior of the energy gap of strained semimetallic zigzag SWNTs as a function of the axial strain up to $\sim 3\%$ strain. We found that this linear behavior is independent of the diameter of the SWNTs. Furthermore, we determined that for $\sigma < \sigma_{\text{crit}}$ where σ_{crit} is the strain where the energy gap of the SWNT vanishes, the slope of the linear relation is ~ -140 meV/% while the slope is ~ 120 meV/% for $\sigma > \sigma_{\text{crit}}$. We have also determined that the observed relatively small changes in the conductance associated with an axial strain but no local perturbation are due to the pinning of the Fermi level in the vicinity of E_V for strained SWNTs contacted by gold leads, even though the strain results in the opening of a substantial energy gap. This pinning is shown to be the consequence of the finite length of the sample SWNTs. Thus, our study has succinctly delineated how the interplay among the strain, the nature of the metallic leads, the pinning of the Fermi level due to the finiteness of the sample SWNTs, and the local perturbation determines the electromechanical responses of SWNTs.

ACKNOWLEDGMENTS

We acknowledge illuminating discussions with Professor, H. Dai. This work was supported by the NSF (DMR-011284 and ECS-0224114), the DOE (DE-FG02-00ER4582), and also National Science Council of Taiwan (NSC 92-2120-M-002-003 and NSC 91-2112-M-054).

- ¹T. W. Tomblor *et al.*, Nature (London) **405**, 769 (2000).
- ²E. D. Minot *et al.*, Phys. Rev. Lett. **90**, 156401 (2003).
- ³L. Liu *et al.*, Phys. Rev. Lett. **84**, 4950 (2000).
- ⁴A. Maiti, A. Svizhenko, and M. P. Anantram, Phys. Rev. Lett. **88**, 126805 (2002).
- ⁵J. Cao, Q. Wang, and H. Dai, Phys. Rev. Lett. **90**, 157601 (2003).
- ⁶R. Heyd, A. Charlier, and E. McRae, Phys. Rev. B **55**, 6820 (1997).
- ⁷L. Yang *et al.*, Phys. Rev. B **60**, 13874 (1999).
- ⁸L. Yang and J. Han, Phys. Rev. Lett. **85**, 154 (2000).
- ⁹P. E. Blöchl, Phys. Rev. B **50**, 17953 (1994); G. Kresse and D. Joubert, *ibid.* **59**, 1758 (1999).
- ¹⁰G. Kresse and J. Hafner, Phys. Rev. B **48**, 13115 (1993); G. Kresse and J. Furthmüller, Comput. Mater. Sci. **6**, 15 (1996); Phys. Rev. B **54**, 11169 (1996).
- ¹¹R. Saito, G. Dresselhaus, and M. S. Dresselhaus, *Physical Properties of Carbon Nanotubes* (Imperial College, London, 1998).
- ¹²M. Ouyang *et al.*, Science **292**, 702 (2001).
- ¹³J. P. Perdew and A. Zunger, Phys. Rev. B **23**, 5048 (1982).
- ¹⁴G. Y. Guo *et al.*, Phys. Rev. B **69**, 205416 (2004).
- ¹⁵C. W. Zhou, J. Kong, and H. Dai, Phys. Rev. Lett. **84**, 5604 (2000).
- ¹⁶P. Keblinski *et al.*, Phys. Rev. Lett. **89**, 255503 (2002).
- ¹⁷F. Léonard and J. Tersoff, Phys. Rev. Lett. **84**, 4693 (2000).
- ¹⁸F. Léonard and J. Tersoff, Phys. Rev. Lett. **85**, 4767 (2000).